



Mechanistic investigation of S_N2 dominated gas phase alkyl iodide reactions

John M. Garver, Nicole Eyet¹, Stephanie M. Villano, Zhibo Yang, Veronica M. Bierbaum*

Department of Chemistry and Biochemistry, University of Colorado, Boulder, CO 80309-0215, United States

ARTICLE INFO

Article history:

Received 8 April 2010

Received in revised form 16 July 2010

Accepted 12 August 2010

Available online 27 August 2010

Keywords:

Gas phase

Ion/molecule

Mechanism

Reactivity

Transition state

Barrier height

ABSTRACT

The competition between substitution (S_N2) and elimination (E2) has been studied for the reactions of methyl, ethyl, isopropyl, and *tert*-butyl iodide with Cl^- , CN^- , and HS^- in the gas phase. Previous studies have shown a dominance of the S_N2 mechanism for sulfur anions and for some cyanide–alkyl iodide reactions. Although our results support this conclusion for the reactions studied, they reveal that competition between the S_N2 and E2 pathways exists for the isopropyl reactions. Steric and electronic effects, upon alkyl group substitution, produce looser and less stable S_N2 transition states, however, they can favor the E2 process. These opposing effects on barrier heights produce E2/ S_N2 competition as steric hindrance increases around the α -carbon, however the relative differences in intrinsic barrier heights lead to significantly different branching ratios. This interpretation is discussed in terms of reaction efficiencies, kinetic isotope effects, linear basicity–reactivity relationships, electrostatic models, and transition state looseness parameters.

Published by Elsevier B.V.

1. Introduction

Studies of bimolecular nucleophilic substitution (S_N2) and base-induced elimination reactions (E2) have made significant contributions to the fundamental knowledge of prototypical organic reactions [1,2] and the conceptual framework for understanding biological systems [3,4]. In these experimental [5–14] and theoretical investigations [15–20], wide-ranging relationships connecting structure and reactivity parameters to reaction rates and mechanistic pathways have been established. These structure–energy relationships form the basis of efforts to predict and control the predominant reaction channel between the two competitive processes. Even within the current conceptual construct, transition state energetics [9,21] and solvent effects [22–25] produce exceptions to expected reactivity and mechanistic selectivity. Of interest for our current research is the apparent dominance of the S_N2 mechanism for sulfur anions [9,21] and for some cyanide–alkyl iodide reactions [26] in the gas phase. By investigating the electronic and structural properties of systems that deviate from typical reactivity patterns, valuable insight can be gained to provide a more detailed picture of kinetics, mechanisms, and product distributions.

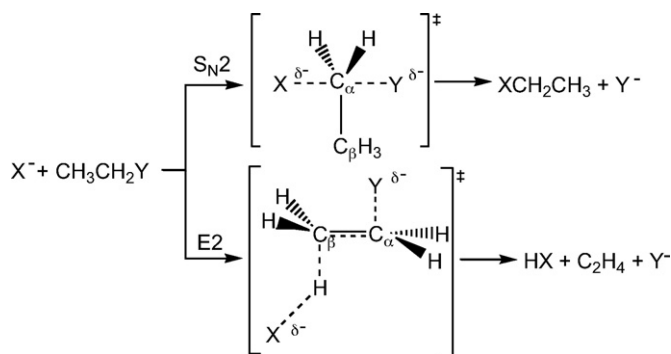
Studies of ion–molecule reactions have shown competition between S_N2 and E2 mechanisms (Scheme 1) to be significantly

influenced by the nature of the attacking group (X^-), leaving group abilities (Y), substrate properties, and solvent effects [9,27–29]. The most influential factors on the E2/ S_N2 ratio are the presence of β -hydrogens, the degree of α - and β -branching, and the nucleophilicity versus basicity of the reactant anion. For an E2 elimination to occur, there must be periplanar β -hydrogens allowing orbital overlap during double bond formation. This sp^3 to sp^2 transformation from reactants to products reduces steric strain between substituents producing a driving force for the E2 process in highly substituted systems. In contrast, increasing alkyl group substitution at the α -carbon or on the attacking group hinders the approach of the nucleophile during the S_N2 process, thus increasing the activation barrier and decreasing contributions from this channel. Experimental investigations into substituent effects around the α -carbon of alkyl halide substrates have shown a transition from predominantly substitution products for primary alkyl halides to exclusively elimination products for tertiary alkyl halides [17,28,30]. In addition to structural influences, strong nucleophilicity (carbon cation affinity measured by kinetics) enhances the S_N2 pathway, while strong basicity (proton affinity measured by thermodynamics) enhances the E2 pathway. Distinguishing between the relative nucleophilic or basic character of an attacking group is not straightforward due to a linear free-energy relationship between these properties. Rationalized in the context of Marcus theory, the intrinsic transition-state barrier height is lowered by the exothermicity of reaction [31,32]. Although gas-phase basicity is often an excellent predictive tool for S_N2 reactivity, deviations in the correlation between S_N2 and E2 barriers arise for attacking atoms outside the same row or group in the periodic table [9,29]. Alternative correlations utilizing transition state geome-

* Corresponding author. Tel.: +1 303 492 7081; fax: +1 303 492 5894.

E-mail address: veronica.bierbaum@colorado.edu (V.M. Bierbaum).

¹ Current address: Department of Chemistry, Saint Anselm College, 100 Saint Anselm Dr. #1760, Manchester, NH 03102, United States.



Scheme 1.

tries, electronegativity, exothermicity and energy barriers have proven insightful [20,33–36].

Intrinsic competition in gas phase ion-molecule reactions probed through mass spectrometry is often used to evaluate structure–energy relationships. However, the ability to differentiate between nucleophilic substitution and base-induced elimination is limited, since the competitive reactions typically produce the same ionic product. While alternate techniques and unique reaction schemes with differentiable products have garnered quantitative information on the competition between S_N2 and E2 pathways [14,28,30], most of the structure–reactivity data have been derived from indirect approaches, such as kinetic isotope effects (KIEs). A deuterium KIE is the ratio of the rate constant for an undeuterated reactant to the rate constant for a particular deuterated reactant ($KIE = k_H/k_D$). Deuterium KIEs enable the structure of the transition state and relative reaction pathways to be probed through relative energy changes in transition-state barrier heights due to isotopic substitution. Since these KIEs are primarily due to changes in the vibrations, a normal KIE (>1) is observed when bonds are loosened on going from reactants to the transition state and an inverse KIE (<1) results from the tightening of bonds on going to the transition state. The magnitude of these effects is sometimes evaluated in terms of transition state “looseness” or “crowdedness” [35].

Numerous groups have employed the use of KIEs derived from theoretical calculations and transition-state theory to elucidate a structural and energetic basis for reactivity [35,37–39]. Various attempts have been made to relate trends in KIEs with the degree of steric crowding on transition-state vibrational energy through a looseness parameter [40–42]. Almost all of these methods have defined the transition-state looseness parameter as a function of nucleophile–leaving group distance. Evaluation of the effectiveness of looseness parameters to predict KIEs indicates that the R_{TS} model (Eq. (1)) works well for S_N2 reactions with the same leaving group [43] and simple monatomic or diatomic nucleophiles [35]:

$$R_{TS} = R_{Nu-C}^{\ddagger} + R_{LG-C}^{\ddagger} \quad (1)$$

where R_{Nu-C}^{\ddagger} refers to the nucleophile– C_{α} bond length at the transition state and R_{LG-C}^{\ddagger} refers to the leaving group– C_{α} bond length at the transition state. In S_N2 processes, the C_{α} –H(D) out-of-plane, bending vibrations will be of higher energy as the looseness parameter decreases contributing to an increased (more inverse) kinetic isotope effect. Studies of ethyl halide reactions indicate that the bending contribution accounts for the magnitude of KIEs in more complex substrates [43].

While the magnitude of the KIE in a reaction that occurs exclusively by S_N2 or by E2 mechanisms can be easily correlated to structure–energy relationships, evaluation of the KIE for a competitive reaction is complicated by contributions from both pathways. Relative contributions can be inferred from the overall KIE as a

fraction of E2 reaction with high deuterium kinetic isotope effects ($k_H/k_D \approx 2$ –6) and a fraction of S_N2 reaction with slightly inverse KIEs ($k_H/k_D \approx 0.7$ –1.0) [18,44]. Such interpretations can be facilitated with a computational KIE for each pathway. Corollary data have also been used to show linear relationships for barrier heights and structural changes with Mulliken charge on the leaving group [36] and with electronegativity of the attacking atom [20]. Assessing these relationships in conjunction with experimental KIEs investigates other factors determining S_N2 and E2 reactivity in addition to basicity.

In this paper, we report on a series of substituted alkyl iodide reactions that display a predominance of the S_N2 mechanism and evaluate structure–energy relationships that correlate with competition between substitution and elimination pathways. We expand our earlier work [26] on alkyl iodide–cyanide ion reactions in the gas phase by investigating the reactions of methyl, ethyl, isopropyl, and *tert*-butyl iodide with hydrogen sulfide and chloride ions. Reactivity patterns are discussed in conjunction with estimated relative barrier heights derived from linear basicity–reactivity relationships. A multipole electrostatic model and transition-state looseness parameters are employed to garner insight into geometric and electronic effects during alkyl group substitution.

2. Experimental

These reactions were carried out in a flowing afterglow–selected ion flow tube (FA-SIFT) mass spectrometer [45]. In the source chamber, chloride and cyanide ions were generated by electron impact on chloroform and cyanogen bromide, respectively, and hydrogen sulfide ions were produced by electron impact on a mixture of carbon disulfide and methane. The reactant anions were then mass selected using a quadrupole mass filter, and injected into the reaction flow tube where they become equilibrated to room temperature through collisions with He buffer gas (~ 0.5 torr, $\sim 10^4$ cm s $^{-1}$). A known flow of neutral reagents was added to the reaction flow tube through a series of fixed inlets at various distances along the flow tube, and the depletion of the reactant ion and formation of the product ions were monitored using a detection quadrupole mass filter coupled to an electron multiplier. Reaction rate constants were determined under pseudo-first order conditions, where the concentration of the alkyl halide ($\sim 10^{11}$ molecules cm $^{-3}$) was significantly greater than the concentration of the reactant ion ($\sim 10^5$ ions cm $^{-3}$). The reactant ion signal (intensities of 10^4 – 10^5 counts s $^{-1}$ with noise levels of ~ 1 count s $^{-1}$) was monitored as the position of the neutral reagent addition was varied, thereby changing the reaction distance and time. The reaction rate constant is obtained from the slope of a plot of the \ln [ion counts] as a function of the neutral reaction distance and other measured experimental parameters; the measured ion decay was at least one order of magnitude. Reported rate constants are the averages of at least three individual measurements.

Absolute uncertainties in these rate measurements are $\pm 20\%$, however some systematic errors (pressure, temperature, He flow rate, etc.) are cancelled in the rate constant ratio, so that the error bars for KIEs are significantly smaller. Neutral reagents [CH_3I , Aldrich 99.5%; CD_3I , Cambridge Isotope Laboratories 99.5% D; CH_3CH_2I , Aldrich 99%; CD_3CD_2I , Isotec 99.5% D; $(CH_3)_2CHI$, Aldrich 99%; $(CD_3)_2CDI$, CDN Isotopes 99.1% D; $(CH_3)_3CI$, Aldrich 95%; $(CD_3)_3CI$, CDN Isotopes 99.5% D] were obtained from commercial vendors and purified by several freeze–pump–thaw cycles before use. The reagents were protected from light and stored under vacuum. Helium buffer gas (99.995%) was purified by passage through a molecular sieve trap immersed in liquid nitrogen. Parallel reactions of deuterated and undeuterated reactants were carried out under identical conditions.

Table 1Reaction rate constants^a (k_H) in units of $10^{-10} \text{ cm}^3 \text{ s}^{-1}$, reaction efficiencies^b (k_H/k_{col}), and isotope effects (KIE_{exp}).

Substrate	Cl^- (Proton Affinity = 333 kcal mol ⁻¹)		HS^- (Proton Affinity = 351 kcal mol ⁻¹)		CN^- ^c (Proton Affinity = 351 kcal mol ⁻¹)	
	k_H (k_H/k_{col})	KIE_{exp}	k_H (k_H/k_{col})	KIE_{exp}	k_H (k_H/k_{col})	KIE_{exp}
Methyl iodide	1.42 ± 0.01 (0.072)	0.86 ± 0.01	6.39 ± 0.03 (0.316)	1.03 ± 0.03	1.28 ± 0.03 (0.057)	0.84 ± 0.03
Ethyl iodide	2.74 ± 0.02 (0.120)	0.96 ± 0.02	7.52 ± 0.20 (0.320)	0.99 ± 0.03	0.30 ± 0.02 (0.012)	0.89 ± 0.02
<i>i</i> -Propyl iodide	0.42 ± 0.01 (0.019)	1.29 ± 0.03	2.60 ± 0.03 (0.101)	1.05 ± 0.05	<0.01	
<i>t</i> -Butyl iodide	0.77 ± 0.02 (0.030)	2.61 ± 0.10	5.35 ± 0.07 (0.204)	1.91 ± 0.04	0.11 ± 0.01 (0.004)	>8 ^d

^a Error bars represent one standard deviation of the mean of 3 or more measurements; absolute accuracy is $\pm 20\%$.^b Efficiency is the ratio of the experimental rate constant to the collision rate constant calculated using parameterized trajectory collision theory [53].^c Previously reported values [26].^d This value is a lower limit without corrections for trace association products and mass discrimination.

3. Computational methods

Electronic structure calculations were carried out using the Gaussian 03 [46] suite of programs to provide additional insight into the experimental results. The MP2/6-311++G(2d,p) level of theory [47–49] for C, N, and H and the LanL2DZ effective core potential [50] for I were employed based on accurate correlations of $\text{S}_{\text{N}}2$ KIEs for the methyl iodide–cyanide ion reaction in previous work [26]. Since optimal scaling factors for similar theoretical methods have zero point vibrational energy, enthalpy, and entropy scaling factors near unity [51], scaling was not employed. Transition states were determined by the existence of one imaginary frequency along the reaction coordinate. The KIEs were calculated using transition-state theory, neglecting any variational or tunneling effects:

$$\frac{k_H}{k_D} = \exp \left(\frac{\Delta G_D^\ddagger - \Delta G_H^\ddagger}{RT} \right) \quad (2)$$

where $\Delta G^\ddagger = G^\ddagger - G^r$. (ΔG^\ddagger is the difference between the zero point corrected free-energy of the transition state relative to the separated reactants). The k_H/k_D ratio for the $\text{S}_{\text{N}}2$ and E2 transition states provides a predicted KIE for each pathway. The $\text{S}_{\text{N}}2$ branching fraction ($\text{BR}_{\text{S}_{\text{N}}2} = k_{\text{S}_{\text{N}}2} / (k_{\text{S}_{\text{N}}2} + k_{\text{E}2})$) was determined using transition-state theory and the ratio of the theoretical rate constants for the perprotio reactions. All frequencies are treated using the harmonic approximation. Although the harmonic treatment of low-frequency modes can introduce error into the entropy term of the free-energy, this effect appears to be minimized in our $\text{S}_{\text{N}}2$ KIE calculations due to the relatively small changes in the lowest frequencies upon isotopic substitution. Charges were calculated by natural population analysis (NPA) at the same level of theory on the optimized geometries.

4. Results and discussion

The experimental rate constants, reaction efficiencies, and deuterium KIEs for the gas phase reactions of chloride, hydrogen sulfide, and cyanide ions with a series of alkyl iodides are given in Table 1. The results for methyl iodide are consistent with previously reported rates and KIEs [52]. With the exception of the reaction of CN^- with isopropyl iodide, the reaction rate constants are within the detectable range of 10^{-9} to $10^{-12} \text{ cm}^3 \text{ s}^{-1}$ for our FA-SIFT. Due to variations in collision rates, reaction efficiencies ($k_{\text{rxn}}/k_{\text{col}}$, where k_{col} is calculated using parameterized trajectory theory [53]) are employed in comparisons. These values represent the fraction of collisions that result in a reaction. The efficiencies are well below the collision-controlled limit indicating the ability to reflect relative differences in barrier heights (ΔG^\ddagger); thus, the rate constants and measured KIEs reflect structure–reactivity differences in the reactions. Both $\text{S}_{\text{N}}2$ and E2 pathways are energetically accessible (see supporting information) for all reactions. Although CN^- is an

ambident nucleophile, the $\text{S}_{\text{N}}2$ and E2 pathways forming nitrile products are thermodynamically favored and assumed to occur exclusively. Recent work [54,55] has discussed the role of single-electron-transfer (SET) character in $\text{S}_{\text{N}}2$ transition states. While an analysis of this relationship for our reaction efficiencies versus ionization potentials suggests trends, the limited data do not allow a complete evaluation of SET.

4.1. Reactivity trends

Since the reactions with methyl halides only proceed by the $\text{S}_{\text{N}}2$ pathway, a comparison of the reactivity of different nucleophiles provides a direct evaluation of nucleophilicity in terms of methyl cation affinity. The experimental ordering of efficiencies was found to be $\text{HS}^- > \text{Cl}^- > \text{CN}^-$. Proton affinities provide a measure of gas-phase basicity for correlations with reactivity. While the relative reactivity of HS^- and Cl^- follows a linear free-energy relationship with Brønsted-type basicity (see Fig. 1a), this correlation breaks down for CN^- . This reduced reactivity relative to basicity can be attributed to the delocalized charge on the attacking anion and the required reorganization of charge densities in the transition state influencing the barrier height. It is worth noting the possible alpha-nucleophilic nature of CN^- (an enhanced reactivity of nucleophiles with a lone pair of electrons adjacent to the attacking atom) is not observed here. This result is perhaps expected since, unlike most alpha-nucleophiles, the lone electron pair in CN^- is isolated from the nucleophilic site by the presence of the triple bond.

The relative correlation of basicity and E2 barrier heights can be accessed from the *tert*-butyl iodide reactions since they have previously been shown to be dominated by the E2 mechanism [9]. The experimental ordering of efficiencies was found to be $\text{HS}^- > \text{Cl}^- > \text{CN}^-$. Once again the reactivity of CN^- is below that expected for the associated basicity (see Fig. 1b). Although similar trends in relative reactivity and Brønsted-type basicity are observed for both the $\text{S}_{\text{N}}2$ and E2 processes, comparison of the slopes for the halide anion with methyl iodide reactions (0.0334) and *tert*-butyl iodide reactions (0.0348) reactions suggest that the E2 barrier is slightly more sensitive to basicity. Computational studies by Ren and Yamataka show a similar trend for competing barriers in $\text{CH}_3\text{CH}_2\text{Cl}$ reactions [56]. If the minor difference in slopes is interpreted as a reflection of the trends in barrier heights, the relative E2 to $\text{S}_{\text{N}}2$ efficiency increases at higher basicities (i.e., more similar $\text{S}_{\text{N}}2$ and E2 barrier heights). Analysis of the ratio of $\text{E}2/\text{S}_{\text{N}}2$ (i.e., $t\text{-C}_4\text{H}_9\text{I}/\text{CH}_3\text{I}$) efficiencies shows an increase from Cl^- (41.7%) to F^- (60.1%). This relationship suggests that the $\text{S}_{\text{N}}2$ and E2 barriers for alkyl iodide reactions are not equivalent until extremely high anion basicities. If these trends in $\text{E}2/\text{S}_{\text{N}}2$ barrier heights apply across the competitive series of ethyl and isopropyl iodide reactions, the $\text{S}_{\text{N}}2$ process should be the prominent pathway for all the nucleophiles in this study. This dominance of the $\text{S}_{\text{N}}2$ pathway is observed in dianion research with ethyl and isopropyl iodides by

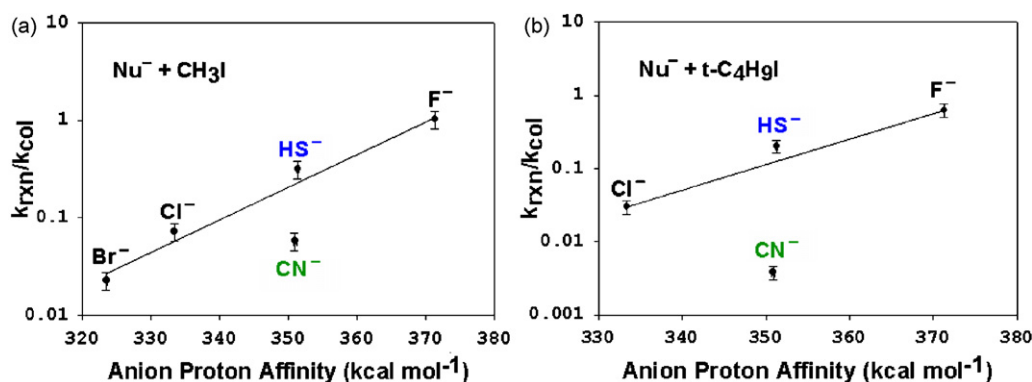


Fig. 1. The logarithm of reaction efficiency ($k_{\text{rxn}}/k_{\text{col}}$) at 298 K versus the anion proton affinity (ΔH_{298}) for (a) the $\text{S}_{\text{N}}2$ reaction of Nu^- with CH_3I and (b) the $\text{E}2$ reaction of Nu^- with $t\text{-C}_4\text{H}_9\text{I}$. The linear trends are fit to the monatomic halide anions due to stronger linear correlations with basicity [20,29,54,55] ($\text{S}_{\text{N}}2$: $y = 0.0334x - 12.39$; $r^2 = 0.989$ and $\text{E}2$: $y = 0.0348x - 13.13$). Experimental data from this work and Ref. [52] updated using parameterized trajectory theory [53] to calculate k_{col} . The reaction rate constant for F^- with $t\text{-C}_4\text{H}_9\text{I}$ was measured as $2.09 (\pm 0.02) \times 10^{-9}$ (this work where the error bars represent one standard deviation of the mean of 3 or more measurements; absolute accuracy is $\pm 20\%$); the reaction of Br^- with $t\text{-C}_4\text{H}_9\text{I}$ is not energetically accessible. Proton affinity data are from [58]. Error bars for the plot represent an absolute accuracy of $\pm 20\%$ in efficiency.

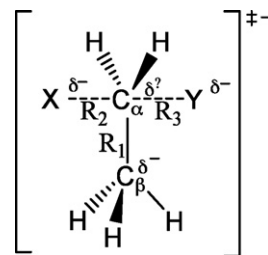
Gronert et al. [28]. Further comparisons show that the CH_3I reaction efficiency of CN^- (0.057) is a factor of 5 below that of HS^- (0.316). However, the $t\text{-C}_4\text{H}_9\text{I}$ reaction efficiency of CN^- (0.004) is a factor of 50 below that of HS^- (0.204), a much greater deviation than in the $\text{S}_{\text{N}}2$ process. This result indicates that variations in electronic and structural changes for the CN^- reaction are magnified in the $\text{E}2$ transition state and that the $\text{E}2$ pathway is even more inhibited in these reactions.

Competing pathways as well as substituent effects complicate the analysis of the reactivity trends of the methyl, ethyl, isopropyl, and *tert*-butyl iodide reactions. Therefore, established trends and a holistic approach must be employed. As C_α -branching increases, $\text{S}_{\text{N}}2$ processes will be inhibited and $\text{E}2$ processes will be enhanced. A decrease in reactivity down the series of alkyl iodides (i.e., $1^\circ \geq 2^\circ \geq 3^\circ$) would be indicative of large $\text{E}2$ barriers and a resulting dominance of the $\text{S}_{\text{N}}2$ pathway. In contrast, an increase in reactivity down the series of alkyl iodides (i.e., $1^\circ \leq 2^\circ \leq 3^\circ$) would be indicative of a major $\text{E}2$ contribution to the overall reaction rate. Applying these concepts to the data in Table 1, patterns emerge that support large barriers to the $\text{E}2$ process. For the Cl^- and HS^- nucleophiles, there is an increase in efficiency for the ethyl reaction followed by a sharp decrease for the isopropyl reaction. Although the increased reactivity in the primary iodide could be indicative of an $\text{E}2$ contribution, the sharp decrease for the secondary iodide dissuades this interpretation. Rather, the enhanced efficiency for the Cl^- and HS^- with ethyl iodide reactions is explained by stabilization of the $\text{S}_{\text{N}}2$ transition state through charge delocalization on the additional methyl group. It is more challenging to explain the dramatic decrease in efficiency along the series of alkyl iodides observed for CN^- where the reaction efficiency drops below 2% for the ethyl reaction and continues to drop below the detection limit for the isopropyl reaction. In an effort to understand the anomalies between trends, we employ a slightly modified electrostatic model that has been effectively used by Gronert et al. for β -substituted alkyl halides [57].

Variations in the magnitude of the efficiency between the methyl and ethyl reactions (67% increase for Cl^- , 1% increase for HS^- , and 79% decrease for CN^-), reflect the combined capability of the methyl and attacking groups to shift electron density away from the α -carbon in the transition state. This effect can be understood by applying a multipole electrostatic model [57] where the transition state is represented by the interaction of the partial charge on the attacking group, the leaving group, the β -carbon, and the α -carbon (Scheme 2). While the thermodynamic stability of the products can be reflected in shifts in the position of the geometry and amount

of charge transferred in the transition state (early or late, i.e. reactant like or product like) used in our application of this model, the differences in the heat of reaction between the methyl and ethyl iodide reactions for a given nucleophile are all less than 1 kcal/mol. Therefore, relative variations in reaction efficiency are expected to be dominated by the intrinsic parameters that can be evaluated through bond lengths and the ionic nature of the transition state.

Although methyl groups are commonly considered weak electron donors in solution, in gas phase reactions at saturated carbon centers they have a tendency to be weak electron acceptors [58]. Polarizability effects on anionic centers play a major role in reactivity and the ability to delocalize charge across alkyl groups significantly stabilizes the anionic $\text{S}_{\text{N}}2$ transition state. In the absence of an electron-withdrawing group on the methyl group to remove electron density, the β -carbon will maintain a partial negative charge. As the $\text{S}_{\text{N}}2$ reaction progresses, electron density from the nucleophile must transfer along the reaction coordinate to the leaving group. Depending on the electronegativity of the attacking and leaving groups, the electron density of the transition state can range from a large partial negative charge on $\text{X}^{\delta-}$ and $\text{Y}^{\delta-}$ (strongly electronegative) with a slight positive charge on $\text{C}_\alpha^{\delta+}$ to a moderate partial negative charge on $\text{X}^{\delta-}$ and $\text{Y}^{\delta-}$ (weakly electronegative) with a slight negative charge on $\text{C}_\alpha^{\delta-}$. If a positive charge develops on C_α , attractive forces between $\text{X}^{\delta-}$, $\text{Y}^{\delta-}$, $\text{C}_\beta^{\delta-}$, and $\text{C}_\alpha^{\delta+}$ will significantly stabilize the transition state. On the opposite extreme, a negative charge on C_α generates repulsive forces between $\text{X}^{\delta-}$, $\text{Y}^{\delta-}$, $\text{C}_\beta^{\delta-}$, and $\text{C}_\alpha^{\delta-}$, destabilizing the transition state. Based on the covalent potential electronegativity scale [59] (calculations in supporting information), Cl^- (6.86) has a higher electronegativity than HS^- (5.83) or CN^- (5.74). As a result, more electron density will be shifted away from C_α in the chloride-ethyl iodide transition state leading to the observed enhanced reactivity compared to the chloride-methyl iodide reaction (further elaboration of this point is



Scheme 2.

Table 2

Experimental KIEs compared to computational KIEs and branching fractions.

Reaction	KIE _{exp}	Theoretical				
		KIE _{S_N2(ΔG)}	KIE _{E2(ΔG)}	BR _{S_N2(ΔG)}	KIE _{S_N2(ΔH)}	KIE _{E2(ΔH)}
Cl [−] + CH ₃ I	0.86 (±0.01)	0.87	–	–	0.86	–
Cl [−] + C ₂ H ₅ I	0.96 (±0.02)	0.97	9.50	0.99	1.00	11.0
Cl [−] + <i>i</i> -C ₃ H ₇ I	1.29 (±0.03)	1.05	9.83	0.97	1.08	10.8
Cl [−] + <i>t</i> -C ₄ H ₉ I	2.61 (±0.01)	–	a	0.00	–	9.5
CN [−] + CH ₃ I	0.84 (±0.03)	0.83	–	–	0.80	–
CN [−] + C ₂ H ₅ I	0.89 (±0.02)	0.89	8.43	0.99	0.87	8.13
CN [−] + <i>i</i> -C ₃ H ₇ I	–	0.93	8.72	0.20	0.94	8.41
CN [−] + <i>t</i> -C ₄ H ₉ I	>8	–	b	0.00	–	7.72
HS [−] + CH ₃ I	1.03 (±0.03)	0.94	–	–	0.95	–
HS [−] + C ₂ H ₅ I	0.99 (±0.03)	1.02	9.56	0.99	1.05	10.0
HS [−] + <i>i</i> -C ₃ H ₇ I	1.05 (±0.05)	1.10	9.66	0.62	1.13	10.0
HS [−] + <i>t</i> -C ₄ H ₉ I	1.91 (±0.04)	–	c	0.00	–	9.17

^a27.4 ^b24.4 ^c27.4; these values are not reliable due to contributions from low-frequency modes.

made below in conjunction with the computational atomic charges in Table 3). Electronegativity differences alone cannot explain the significant difference in efficiency between methyl and ethyl iodide reactions for CN[−] and HS[−] which have approximately the same electronegativity. However, if the relative R₁, R₂, R₃ bond distances of the model are taken into account in conjunction with electrostatic effects, shorter bonds would lead to larger repulsive forces and the observed reduced reactivity. A more inverse KIE for CN[−] (KIE = 0.89) versus HS[−] (KIE = 0.99) supports the presence of shorter bonds in the transition state. Therefore, the higher repulsive forces in the cyanide–ethyl iodide transition state would reduce efficiency. While based primarily on electrostatic field effects, this simple model seems to provide an effective explanation for variations in reactivity trends. Application of this model to other reactions is expected to hold, and computational studies by Wu et al. show a strong linear relationship between barrier heights and electronegativity for twelve nucleophiles [20].

In an attempt to further discern the role of competition in these reactions, a qualitative analysis was made using estimated relative free-energy barrier heights from our E2/S_N2 basicity–reactivity linear-fit baselines. To effectively analyze trends in reactivity relative to the free-energy barrier heights a common scale must be employed. Therefore the relative E2 to S_N2 free-energy barrier heights estimated from our E2/S_N2 efficiencies are scaled to the linear S_N2 basicity–reactivity baseline. A qualitative depiction of the relationship of the free-energy barrier heights for and between anions is shown in Fig. 2. The S_N2 free-energy barrier height for HS[−] is slightly below the baseline reflecting slightly higher reactivity and the CN[−] free-energy barrier height is significantly above the baseline reflecting substantially lower reactivity (this correlates directly to Fig. 1a). The E2 transition-state barrier height (ΔG[‡]_{E2}) reflects a rough estimate of the variance between the lowest S_N2 and E2 free-energy barrier heights, which is related to the percent difference in *t*-C₄H₉I and CH₃I reaction efficiencies (%ΔG[‡]_{S_N2} = *t*-C₄H₉I efficiency divided by the CH₃I efficiency, although the linear proportionality is a simplification). While these approximations are based on experimental data, the use of efficiency ratios relies on many assumptions and is only intended to provide a plausible interpretation of branching ratios when used in conjunction with efficiencies and KIEs.

Upon transitioning from the methyl to the *tert*-butyl iodide reactions, each additional methyl group will generate steric effects increasing the S_N2 free-energy barriers towards and above the E2 free-energy barriers. Examining the series of reactions in the context of these effects on the free-energy barrier heights, the S_N2 process is expected to dominate in the ethyl reactions with perhaps a small contribution of the E2 channel for HS[−]. In the case of isopropyl, we would expect a small contribution of the E2 channel

for Cl[−], competitive contributions from both the S_N2 and E2 channels for HS[−], and extremely small contributions from either channel for CN[−] due to the high free-energy barriers for both channels. In the *tert*-butyl reactions, significant steric hindrance will drive all the S_N2 free-energy barriers to be higher than the E2 free-energy barriers. The E2 mechanism will dominate; however, due to the higher E2 free-energy barrier for CN[−] the efficiency would remain extremely low. The efficiencies and KIEs are in agreement with this assessment suggesting that the relationship between free-energy barrier heights established by the basicity–reactivity baselines is reasonable.

4.2. Kinetic isotope effects

If deuterium KIEs are used to rationalize the mechanisms for all three sets of anion reactions, the results also indicate a predominance of the S_N2 pathway for the ethyl and isopropyl iodides. Across the methyl iodide reactions, the KIEs are inverse or near unity reflecting the expected vibrational changes during sp³ → sp² hybridization in an S_N2 transition state. This trend continues for the ethyl iodides indicating that the substitution channel is the dominant factor in the total KIE. The more normal effect for HS[−] with methyl halides has been attributed to a small inverse vibrational contribution and a more normal rotational contribution (high moment of inertia due to larger size and higher mass) to the overall KIE [35]. This “loose” S_N2 transition state explains the relatively constant KIE (0.99–1.05) for the HS[−] with methyl, ethyl, and isopropyl iodide series. It is not until the tertiary iodides that KIEs associated with the E2 channel are observed in all reactions.

A KIE significantly larger (>8) than predicted by semi-classical theory (≈7) is observed for the CN[−] with *tert*-butyl iodide reaction. This value is established as a lower limit and is most likely higher due to mass discrimination and trace association products. The ability to more accurately assess the magnitude of this effect with confidence is limited by a combination of the larger error associated with smaller ion-signal changes due to the low reactivity and the high mass of the products. KIEs larger than the theoretical limit may be evidence of quantum mechanical tunneling, however alternate explanations have been offered by Gronert et al. [14] for observed KIEs of this magnitude in the gas phase. In reactions with barriers near the entrance channel, the pathways with the greater deuterium barrier height (≈1 kcal mol^{−1}) are influenced by the lifetime of the collision complex leading to significantly lower rates. In reactions with competing pathways, a shift in barrier heights could push the deuterated system towards the S_N2 pathway. This explanation is interesting in light of the apparent dominance of the S_N2 channel in the ethyl and isopropyl iodide systems, but further discussion is beyond the scope of this paper.

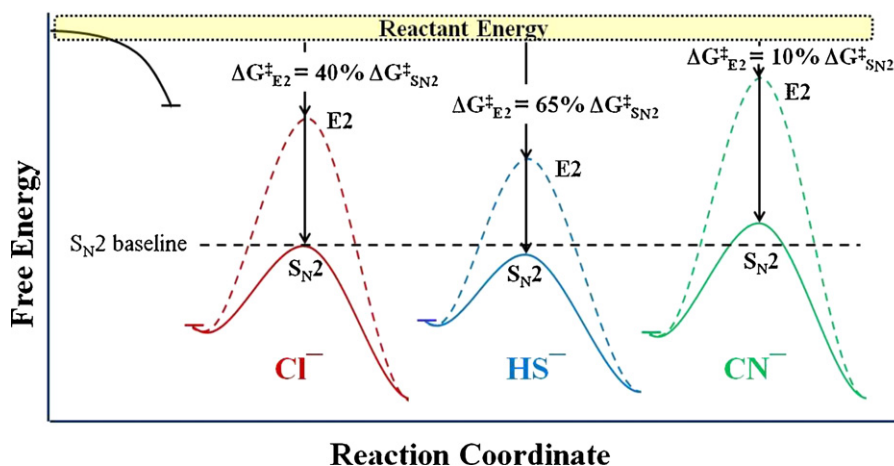


Fig. 2. Qualitative depiction of relative S_N2 barrier heights for CH_3I and the $E2$ barrier heights for $t\text{-C}_4\text{H}_9I$ estimated from the basicity–reactivity baselines of Fig. 1. The black dashed line (—) represents the linear fit of the S_N2 basicity–reactivity baseline.

4.3. Computational work

While higher levels of theory might improve the quantitative accuracy of the reaction barriers (see [supporting information](#)), our focus is on qualitative comparisons to experimental data. Therefore, our methodology only employs quantitative ratios of energies and discusses trends in geometry and charge distribution, which are less sensitive to the level of theory employed. To facilitate these comparisons, the isotope effect was computed using differences in enthalpy and free-energy, as well as an estimate of the S_N2 branching fraction ($BR_{S_N2(\Delta G)}$) based on relative computational free-energy changes. Table 2 provides a summary of the results. Interpretation of the theoretical KIEs in the table should be tempered with an understanding of the calculations. As alkyl substitution increases, so do the number of low-frequency modes associated with the reactants and transition states. These low frequencies are difficult to model and can introduce error, especially in the entropic contribution to the free-energy. However, this inaccuracy is minimized by small relative differences in the low-frequency modes between the perprotio and perdeuterio reactions cancelling in the energy ratios. Reasonably good agreement between the free-energy (ΔG) and enthalpy (ΔH) computational KIEs for the series of alkyl iodide reactions was obtained, which indicates that significant variations in the low-frequency modes do not occur except for the *tert*-butyl iodide reactions. Although general comments can be made about the *tert*-butyl iodide reactions, deviations between the experimental data and the *tert*-butyl iodide calculations prevent the correlation of trend data. Since the experimental reactivity is governed by free-energy barriers, further discussions of KIEs will employ the free-energy computational values.

Reasonably good agreement of the computational $KIE_{S_N2(\Delta G)}$ with the experimental S_N2 KIEs and estimated product distributions indicates that the theoretical level is adequate for qualitative analysis and R_{TS} comparisons for the methyl, ethyl and isopropyl iodide reactions. Calculating the expected total KIE using the magnitude of the theoretical KIEs and estimated branching ratio for the Cl^- with isopropyl iodide reaction ($KIE_{tot} = KIE_{E2(\Delta G)} \times BR_{E2(\Delta G)} + KIE_{S_N2(\Delta G)} \times BR_{S_N2(\Delta G)}$), gives a value of $KIE_{tot} = 1.31$. When compared to the $KIE_{exp} = 1.29$, this combination of branching ratios and magnitudes of KIEs seems viable. In contrast, meaningful branching ratios for the *tert*-butyl iodide reactions cannot be deduced from the computational KIEs due to their limited reliability. However, based on the large computational KIEs for all the $E2$ reactions the low KIE_{exp} for the reactions of Cl^- and HS^- with *tert*-butyl iodide pose the intriguing possibility of minor S_N2 contributions to these processes.

The $BR_{S_N2(\Delta G)}$, as calculated from transition-state theory and summarized in Table 2, support large contributions from the S_N2 channel in the primary and secondary iodides, but no contribution in the tertiary iodide. It is interesting to note the computed branching fractions relative to the efficiency trends observed in the reaction. Upon switching from ethyl to isopropyl iodide, the efficiency of the Cl^- reaction decreases by 90%, while the efficiency of the HS^- reaction only decreases by 30%. The predicted S_N2 and $E2$ branching provide an interpretation of this effect based on two factors. First, the increase in steric hindrance around the α -carbon significantly inhibits the S_N2 process. Second, the $E2$ process is competitive for HS^- allowing a contribution to the overall rate from this channel. Our correlation of $E2/S_N2$ barrier heights with basicity inferred from our $t\text{-C}_4\text{H}_9I/CH_3I$ efficiency ratios supports the $E2$ channel being more competitive for the more basic HS^- .

4.4. Looseness parameters and electrostatic model

Correlations between experimental KIEs and looseness parameters have been primarily restricted to methyl and *tert*-butyl halide reactions in the gas phase. Expansion of these concepts to the S_N2 dominated ethyl and isopropyl iodide reactions provides new insight into transition-state structures upon substitution. The looseness parameter (R_{TS}), theoretical S_N2 KIEs, and transition state α -carbon atomic charge are compiled in Table 3 for the S_N2 reactions. Although specific values are listed in the table, these numbers are not considered an actual measure of the molecular structures or charge. Rather, the parameters are interpreted qualitatively in order to access overall trends.

A key observation in Table 3 is a loosening of the transition states upon α -carbon substitution. A comparison of R_{TS} and KIE_{exp} clearly shows an increasingly normal isotope effect corresponding to longer bonds in the transition state upon progression from methyl through isopropyl iodide. This change in isotope effect could also be attributed to a reduction in the number of α -hydrogen/deuterium. However, scaling the isotope effect relative to the number of hydrogens does not fully account for the magnitude of the shift. Experimental condensed phase data have correlated looser S_N2 transition states for ethyl ($KIE \geq 1$) compared to methyl ($KIE \leq 1$) reactions [42]. Even more compelling experimental evidence for larger (more normal) isotope effects and looser transition states (longer bonds) is the shift from inverse to normal S_N2 KIEs for ethyl to isopropyl dianion reactions in the gas phase [14]. Connecting these effects between the condensed and gas phase further

Table 3

Looseness parameter (R_{TS})^a, theoretical S_N2 KIEs, and transition state α -carbon atomic charge^b.

S_N2 reaction	R_{TS}	KIE $_{S_N2}(\Delta G)$	C_α^δ
$Cl^- + CH_3I$	4.93	0.87	−0.2
$Cl^- + C_2H_5I$	5.02	0.97	0.0
$Cl^- + i-C_3H_7I$	5.15	1.05	0.4
$CN^- + CH_3I$	4.71	0.83	−0.3
$CN^- + C_2H_5I$	4.77	0.89	−0.1
$CN^- + i-C_3H_7I$	4.86	0.93	0.3
$HS^- + CH_3I$	4.75	0.94	−0.3
$HS^- + C_2H_5I$	5.07	1.02	−0.1
$HS^- + i-C_3H_7I$	5.17	1.10	0.3

^a Units of Å.

^b Natural charge distribution (units of elemental charge, e) in terms of Natural Population Analysis (NPA) calculations at the MP2/6-311++G(2d,p) level of theory for C, N, and H and the LanL2DZ effective core potential for I on the transition state geometries.

substantiates the recent use of KIEs to assess significantly tighter transition states in the gas phase versus solution.

Application of the electrostatic model [57] in conjunction with the electronegativity of the nucleophiles and R_{TS} to evaluate relative reactivity is bolstered by the trends in charge density predicted by NPA calculations. The transition states exhibit similar delocalization of charge upon alkyl group substitution on the α -carbon. However, in the ethyl iodide reaction, the more electronegative Cl^- shifts enough electron density away from the α -carbon to significantly reduce repulsive forces and stabilize the transition state. Based on a higher charge density on the α -carbon, tighter transition states ($R_{TS} = R_1 + R_2$) for CN^- have higher repulsive forces, which destabilize the transition state.

While this model predicts an even more stable transition state for the isopropyl reactions, the reduced efficiency indicates that other factors are destabilizing the transition state. An obvious feature absent in the model when applied across substrates is the effect of steric factors. Alkyl substitution generates steric hindrance which can suppress the S_N2 process, while the release of steric strain in branched substrates can favor the E2 reaction. These forces have the ability to drive changes in relative barrier heights and influence branching ratios. For the reactions studied, the steric and electronic effects do not display the ability to drive large deviations from the original E2/ S_N2 ratios established using the basicity–reactivity baseline. As a result computational branching ratios could be employed with estimated relative barrier heights to correlate reaction efficiencies for the different anions.

One final note of interest, when reviewing the atomic charges present in the transition states there is significantly more charge on the leaving group for the reaction of Cl^- and isopropyl iodide reaction, than for the analogous reactions. This is intriguing because the S_N2 process is predicted to dominate the branching ratio for this reaction relative to the other anions. Computational studies [60] have shown enhanced reactivity (lower S_N2 barrier heights) for nucleophiles with looser and more ionic transition states (i.e., $X^{\delta-}$, $Y^{\delta-}$, and $C_\alpha^{\delta+}$), such as those present in the Cl^- and isopropyl iodide reaction.

5. Conclusion

Our investigation of the apparent dominance of the S_N2 mechanism for some alkyl iodide reactions has provided a more detailed picture of kinetics, mechanisms, and product distributions in the gas phase. Analysis of reactivity trends and the electronic and structural properties for the series of alkyl iodide reactions with Cl^- , HS^- , and CN^- have led to the following findings.

- (1) The relative E2/ S_N2 barrier heights for the ethyl and isopropyl iodide reactions appear to significantly favor the S_N2 pathway. Relative efficiencies indicate that the E2 pathway is more sensitive to basicity. At higher anion basicities the E2 pathway becomes more competitive with the S_N2 process.
- (2) A multipole electrostatic model [57] explains the relative reactivity for reactions with similar branching and steric factors. When employed in conjunction with the electronegativity of the nucleophile (to account for electron density on C_α) and the looseness of the transition state (assessed through KIEs or R_{TS}), all trends in the ethyl iodide reactions can be explained.
- (3) Larger (more normal) isotope effects and looser S_N2 transition states (longer bonds) are produced upon alkyl group substitution. These effects correlate with condensed phase studies.

The alkyl iodide reaction series has proven to be an ideal system for expansion of common techniques for evaluating exclusively S_N2 reactions and correlating the results of dianion studies. The halide ion–alkyl iodide reactions provide a simple monatomic basicity–reactivity baseline from which reactivity changes for various nucleophiles can be assessed. In addition, the reaction rate constants fall within the center of our experimental detection range. Future gas-phase studies on alkyl iodide reactions are certain to provide further insight into reactivity trends.

Acknowledgements

We are pleased to dedicate this paper to Prof. Michael L. Gross, a superb scientist and an esteemed colleague. The authors gratefully acknowledge support of this work by the National Science Foundation (CHE 0647088) and the AFOSR (FA9550-09-1-0046). JMG respectfully acknowledges the sponsorship and support of the Air Force Institute of Technology. The computational work was supported by an allocation through the TeraGrid Advanced Support Program. We appreciate the insightful discussions with Professor Charles H. DePuy and Professor Eric Patterson.

Appendix A. Supplementary data

Supplementary data associated with this article can be found, in the online version, at doi:10.1016/j.ijms.2010.08.008.

References

- [1] F.A. Carey, R.J. Sundberg, *Advanced Organic Chemistry: Part A: Structure and Mechanism*, 5th ed., Springer, New York, 2007.
- [2] T.H. Lowry, K.S. Richardson, *Mechanism and Theory in Organic Chemistry*, Harper and Row, New York, 1987.
- [3] S.M. Bachrach, D.C. Mulhearn, Nucleophilic substitution at sulfur: $S(N)2$ or addition–elimination? *Journal of Physical Chemistry* 100 (1996) 3535–3540.
- [4] O. Dmitrenko, C. Thorpe, R.D. Bach, Mechanism of S_N2 disulfide bond cleavage by phosphorus nucleophiles. Implications for biochemical disulfide reducing agents, *Journal of Organic Chemistry* 72 (2007) 8298–8307.
- [5] R.C. Lum, J.J. Grabowski, The intrinsic competition between elimination and substitution mechanisms is controlled by nucleophile structure, *Journal of the American Chemical Society* 114 (1992) 9663–9665.
- [6] B.D. Wladkowski, J.I. Brauman, Substitution versus elimination in gas-phase ionic reactions, *Journal of the American Chemical Society* 114 (1992) 10643–10644.
- [7] S.M. Villano, N. Eyet, W.C. Lineberger, V.M. Bierbaum, Reactions of alpha-nucleophiles with alkyl chlorides: competition between $S(N)2$ and E2 mechanisms and the gas-phase alpha-effect, *Journal of the American Chemical Society* 131 (2009) 8227–8233.
- [8] S.M. Villano, S. Kato, V.M. Bierbaum, Deuterium kinetic isotope effects in gas-phase $S(N)2$ and E2 reactions: comparison of experiment and theory, *Journal of the American Chemical Society* 128 (2006) 736–737.
- [9] C.H. DePuy, S. Gronert, A. Mullin, V.M. Bierbaum, Gas-phase S_N2 and E2 reactions of alkyl-halides, *Journal of the American Chemical Society* 112 (1990) 8650–8655.
- [10] S. Gronert, Gas phase studies of the competition between substitution and elimination reactions, *Accounts of Chemical Research* 36 (2003) 848–857.

- [11] J. Haib, D. Stahl, Competition between substitution (S_N2), elimination (E2) and addition elimination (AE) reactions in the gas-phase, *Organic Mass Spectrometry* 27 (1992) 377–382.
- [12] R.C. Lum, J.J. Grabowski, Substitution competes with elimination in a gas-phase anion molecule reaction, *Journal of the American Chemical Society* 110 (1988) 8568–8570.
- [13] M.E. Jones, G.B. Ellison, A gas-phase E2 reaction—methoxide ion and bromopropane, *Journal of the American Chemical Society* 111 (1989) 1645–1654.
- [14] S. Gronert, A.E. Fagin, L. Wong, Direct measurements of deuterium kinetic isotope effects in anionic, gas-phase substitution and elimination reactions, *Journal of the American Chemical Society* 129 (2007) 5330–5331.
- [15] M. Mugnai, G. Cardini, V. Schettino, Substitution and elimination reaction of F^- with C_2H_5Cl : an ab initio molecular dynamics study, *Journal of Physical Chemistry A* 107 (2003) 2540–2547.
- [16] L.V. Ermolaeva, S.A. Appolonova, V.V. Plemenkov, A.I. Kononov, Gas phase reaction of F^- with chlorocyclopropane. Ab initio study of elimination and substitution, *Theochem-Journal of Molecular Structure* 398 (1997) 451–455.
- [17] S. Gronert, C.H. DePuy, V.M. Bierbaum, Deuterium-isotope effects in gas-phase reactions of alkyl-halides—distinguishing E2 and S_N2 pathways, *Journal of the American Chemical Society* 113 (1991) 4009–4010.
- [18] W.P. Hu, D.G. Truhlar, Factors affecting competitive ion-molecule reactions: $ClO^- + C_2H_5Cl$ and C_2D_5Cl via E2 and $S(N)2$ channels, *Journal of the American Chemical Society* 118 (1996) 860–869.
- [19] F.M. Bickelhaupt, Understanding reactivity with Kohn–Sham molecular orbital theory: E2- $S(N)2$ mechanistic spectrum and other concepts, *Journal of Computational Chemistry* 20 (1999) 114–128.
- [20] X.P. Wu, X.M. Sun, X.G. Wei, Y. Ren, N.B. Wong, W.K. Li, Exploring the reactivity trends in the E2 and $S(N)2$ reactions of $X^- + CH_3CH_2Cl$ ($X = F, Cl, Br, HO, HS, HSe, NH_2, PH_2, AsH_2, CH_3, SiH_3$, and GeH_3), *Journal of Chemical Theory and Computation* 5 (2009) 1597–1606.
- [21] S. Gronert, J.M. Lee, Gas-phase reactions of methyloxirane with HO^- and methylthiirane with HO^- and HS^- . An ab-initio study of addition and elimination, *Journal of Organic Chemistry* 60 (1995) 4488–4497.
- [22] G.I. Mackay, D.K. Bohme, Bridging the gap between gas-phase and solution—transition in relative acidity of water and methanol at 296 ± 2 K, *Journal of the American Chemical Society* 100 (1978) 327–329.
- [23] W.N. Olmstead, J.I. Brauman, Gas-phase nucleophilic displacement-reactions, *Journal of the American Chemical Society* 99 (1977) 4219–4228.
- [24] R.A.J. O'Hair, G.E. Davico, J. Hacaloglu, T.T. Dang, C.H. DePuy, V.M. Bierbaum, Measurements of solvent and secondary kinetic isotope effects for the gas-phase $S(N)2$ reactions of fluoride with methyl halides, *Journal of the American Chemical Society* 116 (1994) 3609–3610.
- [25] M.M. Toteva, J.P. Richard, Structure–reactivity relationships for addition of sulfur nucleophiles to electrophilic carbon: resonance, polarization, and steric/electrostatic effects, *Journal of the American Chemical Society* 122 (2000) 11073–11083.
- [26] J.M. Garver, Y. Fang, N. Eyet, S.M. Villano, V.M. Bierbaum, K.C. Westaway, A direct comparison of reactivity and mechanism in the gas phase and solution, *Journal of the American Chemical Society* 132 (2010) 3808–3814.
- [27] E. Uggerud, Steric and electronic effects in $S(N)2$ reactions, *Pure and Applied Chemistry* 81 (2009) 709–717.
- [28] S. Gronert, A.E. Fagin, K. Okamoto, S. Mogali, L.M. Pratt, Leaving group effects in gas-phase substitutions and eliminations, *Journal of the American Chemical Society* 126 (2004) 12977–12983.
- [29] S. Gronert, Mass spectrometric studies of organic ion/molecule reactions, *Chemical Reviews* 101 (2001) 329–360.
- [30] A.E. Flores, S. Gronert, The gas-phase reactions of dianions with alkyl bromides: direct identification of $S(N)2$ and E2 products, *Journal of the American Chemical Society* 121 (1999) 2627–2628.
- [31] M.J. Pellerite, J.I. Brauman, Intrinsic barriers in nucleophilic displacements—a general-model for intrinsic nucleophilicity toward methyl centers, *Journal of the American Chemical Society* 105 (1983) 2672–2680.
- [32] J.K. Laerdahl, E. Uggerud, Gas phase nucleophilic substitution, *International Journal of Mass Spectrometry* 214 (2002) 277–314.
- [33] S.S. Glad, F. Jensen, Kinetic isotope effects and transition state geometries. A theoretical investigation of E2 model systems, *Journal of Organic Chemistry* 62 (1997) 253–260.
- [34] P.A. Nielsen, S.S. Glad, F. Jensen, Influence of substituents on kinetic isotope effects, *Journal of the American Chemical Society* 118 (1996) 10577–10583.
- [35] G.E. Davico, V.M. Bierbaum, Reactivity and secondary kinetic isotope effects in the $S(N)2$ reaction mechanism: dioxygen radical anion and related nucleophiles, *Journal of the American Chemical Society* 122 (2000) 1740–1748.
- [36] S.S. Glad, F. Jensen, Inference of transition-state geometries from kinetic isotope effects—an Ab-Initio Study of an E2 model system, *Journal of the American Chemical Society* 116 (1994) 9302–9310.
- [37] A.A. Viggiano, J.S. Paschke, R.A. Morris, J.F. Paulson, A. Gonzalezlafont, D.G. Truhlar, Temperature-dependence of the kinetic isotope effect for a gas-phase S_N2 reaction— $Cl^- + CH_3Br$, *Journal of the American Chemical Society* 113 (1991) 9404–9405.
- [38] W.P. Hu, D.G. Truhlar, Deuterium kinetic isotope effects and their temperature-dependence in the gas-phase S_N2 reactions $X^- + CH_3Y \rightarrow CH_3X + Y^-$ ($X, Y = Cl, Br, I$), *Journal of the American Chemical Society* 117 (1995) 10726–10734.
- [39] W.P. Hu, D.G. Truhlar, Modeling transition-state solvation at the single-molecule level—test of correlated ab-initio predictions against experiment for the gas-phase $S(N)2$ reaction of microhydrated fluoride with methyl-chloride, *Journal of the American Chemical Society* 116 (1994) 7797–7800.
- [40] S.S. Glad, F. Jensen, Transition state looseness and alpha-secondary kinetic isotope effects, *Journal of the American Chemical Society* 119 (1997) 227–232.
- [41] S. Wolfe, C.K. Kim, Secondary H/D isotope effects in methyl-transfer reactions decrease with increasing looseness of the transition structure, *Journal of the American Chemical Society* 113 (1991) 8056–8061.
- [42] R.A. Poirier, Y.L. Wang, K.C. Westaway, A theoretical-study of the relationship between secondary alpha-deuterium kinetic isotope effects and the structure of $S(N)2$ transition-states, *Journal of the American Chemical Society* 116 (1994) 2526–2533.
- [43] K.C. Westaway, Determining transition state structure using kinetic isotope effects, *Journal of Labelled Compounds & Radiopharmaceuticals* 50 (2007) 989–1005.
- [44] S. Gronert, C.H. DePuy, V.M. Bierbaum, Deuterium-isotope effects in gas-phase reactions—distinguishing E2 and S_N2 pathways, *Journal of the American Chemical Society* 113 (1991) 4009–4010.
- [45] J.M. Van Doren, S.E. Barlow, C.H. DePuy, V.M. Bierbaum, The tandem flowing afterglow-SIFT-drift, *International Journal of Mass Spectrometry and Ion Processes* 81 (1987) 85–100.
- [46] M.J. Frisch, G.W. Trucks, H.B. Schlegel, G.E. Scuseria, M.A. Robb, J.R. Cheeseman, J.J.A. Montgomery, T. Vreven, K.N. Kudin, J.C. Burant, J.M. Millam, S.S. Iyengar, J. Tomasi, V. Barone, B. Mennucci, M. Cossi, G. Scalmani, N. Rega, G.A. Petersson, H. Nakatsuji, M. Hada, M. Ehara, K. Toyota, R. Fukuda, J. Hasegawa, M. Ishida, T. Nakajima, Y. Honda, O. Kitao, H. Nakai, M. Klene, X. Li, J.E. Knox, H.P. Hratchian, J.B. Cross, V. Bakken, C. Adamo, J. Jaramillo, R. Gomperts, R.E. Stratmann, O. Yazyev, A.J. Austin, R. Cammi, C. Pomelli, J.W. Ochterski, P.Y. Ayala, K. Morokuma, G.A. Voth, P. Salvador, J.J. Dannenberg, V.G. Zakrzewski, S. Dapprich, A.D. Daniels, M.C. Strain, O. Farkas, D.K. Malick, A.D. Rabuck, K. Raghavachari, J.B. Foresman, J.V. Ortiz, Q. Cui, A.G. Baboul, S. Clifford, J. Cioslowski, B.B. Stefanov, G. Liu, A. Liashenko, P. Piskorz, I. Komaromi, R.L. Martin, D.J. Fox, T. Keith, M.A. Al-Laham, C.Y. Peng, A. Nanayakkara, M. Challacombe, P.M.W. Gill, B. Johnson, W. Chen, M.W. Wong, C. Gonzalez, J.A. Pople, Gaussian 03, Revision B. 05, Gaussian, Inc., Pittsburgh, PA, 2004.
- [47] Q.Z. Zhang, H.N. Wang, T.L. Sun, W.X. Wang, A theoretical investigation for the reaction of CH_3CH_2SH with atomic H: mechanism and kinetics properties, *Chemical Physics* 324 (2006) 298–306.
- [48] C.M. Hadad, P.R. Rablen, K.B. Wiberg, C–O and C–S bonds: stability, bond dissociation energies, and resonance stabilization, *Journal of Organic Chemistry* 63 (1998) 8668–8681.
- [49] C. Moller, M.S. Plesset, Note on an approximation treatment for many-electron systems, *Physical Review* 46 (1934) 0618–0622.
- [50] P.J. Hay, W.R. Wadt, Ab initio effective core potentials for molecular calculations. Potentials for the transition metal atoms Sc to Hg, *Journal of Chemical Physics*, American Institute of Physics (1985) 270.
- [51] J.P. Merrick, D. Moran, L. Radom, An evaluation of harmonic vibrational frequency scale factors, *Journal of Physical Chemistry A* 111 (2007) 11683–11700.
- [52] V.M. Bierbaum, J.J. Grabowski, C.H. DePuy, Gas-phase synthesis and reactions of nitrogen-containing and sulfur-containing anions, *Journal of Physical Chemistry* 88 (1984) 1389–1393.
- [53] T. Su, W.J. Chesnavich, Parametrization of the ion-polar molecule collision rate-constant by trajectory calculations, *Journal of Chemical Physics* 76 (1982) 5183–5185.
- [54] R.R. Sauer, Single electron transfer and $S(N)2$ reactions: the importance of ionization potential of nucleophiles, *Journal of Chemical Theory and Computation* 6 (2010) 602–606.
- [55] S.S. Shaik, The S_N2 and single electron-transfer concepts—a theoretical and experimental overview, *Acta Chemica Scandinavica* 44 (1990) 205–221.
- [56] Y. Ren, H. Yamataka, Does alpha-effect exist in E2 reactions? A $G2(+)$ investigation, *Journal of Computational Chemistry* 30 (2009) 358–365.
- [57] S. Gronert, L.M. Pratt, S. Mogali, Substituent effects in gas-phase substitutions and eliminations: beta-Halo substituents. Solvation reverses $S(N)2$ substituent effects, *Journal of the American Chemical Society* 123 (2001) 3081–3091.
- [58] J. March, *Advanced Organic Chemistry: Reactions, Mechanisms, and Structure*, 4th edition, John Wiley and Sons, New York, 1992.
- [59] Y.R. Luo, S.W. Benson, The covalent potential—a simple and useful measure of the valence-state electronegativity for correlating molecular energetics, *Accounts of Chemical Research* 25 (1992) 375–381.
- [60] Y. Ren, H. Yamataka, The alpha-effect in gas-phase $S(N)2$ reactions: existence and the origin of the effect, *Journal of Organic Chemistry* 72 (2007) 5660–5667.